

# A Diffusion-Based Approach to Geminate Recombination of Heme Proteins with Small Ligands

V. S. Starovoitov<sup>1</sup> and B. M. Dzhangarov<sup>2</sup>

<sup>1</sup> *B.I.Stepanov Institute of Physics, NASB, 220072, Scarina ave. 70, Minsk, Belarus*

<sup>2</sup> *Institute of Molecular and Atomic Physics NASB, 220072, Scarina ave. 70, Minsk, Belarus*

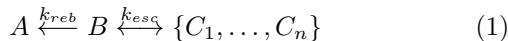
(November 13, 2018)

A model of postphotodissociative monomolecular (geminate) recombination of heme proteins with small ligands ( $NO$ ,  $O_2$  or  $CO$ ) is represented. The non-exponential decay with time for the probability to find a heme in unbound state is interpreted in terms of diffusion-like migration of ligand between protein cavities. The temporal behavior for the probability is obtained from numerical simulation and specified by two parameters: the time  $\tau_{reb}$  of heme-ligand rebinding for the ligand localized inside the heme pocket and the time  $\tau_{esc}$  of ligand escape from the pocket. The model is applied in the analysis of available experimental data for geminate reoxygenation of human hemoglobin  $HbA$ . Our simulation is in good agreement with the measurements. The analysis shows that the variation in  $pH$  of the solution ( $6.0 < pH < 9.4$ ) results in considerable changes for  $\tau_{reb}$  from 0.36 ns (at  $pH = 8.5$ ) up to 0.5 ns ( $pH = 6.0$ ) but effects slightly on the time  $\tau_{esc}$  ( $\tau_{esc} \approx 0.88$  ns).

## I. INTRODUCTION

The binding reactions between myoglobin ( $Mb$ ) or hemoglobin ( $Hb$ ) and small ligands ( $NO$ ,  $O_2$  or  $CO$ ) are objects of extensive investigations during many decades because of the great functional importance of the heme proteins for living systems [1–3]. In the investigations a special attention is paid to the heme-ligand recombination process going after fast photodissociative bond breaking between a ligand molecule and an ion  $Fe^{++}$  located in the center of a heme ( $Fe$ -protoporphyrin IX complex). The kinetic study of the postphotodissociative recombination allows to obtain detailed information on the protein-ligand interaction mechanism, the protein structure, the allosteric effect and the medium influence on the recombination efficiency (see, for example, references [4–9]).

The heme is well-wrapped in protein helices, which prevent the iron from the solvent and hinder the ligand migration through protein matrix. On a sufficiently long time scale (at  $t \leq 100$  ns in the case of  $Hb$ ) after dissociation, when the ligand is not managed to leave the protein and to move significantly away from the parent heme, the recombination is a monomolecular reaction designated usually as a geminate recombination (GR) [5]. Schematically, the GR can be written as [10]:



where  $A$  is the bound heme-ligand state. The substates  $B$  and  $\{C_1, \dots, C_n\}$  form the unbound state. Each of these substates corresponds to ligand localization in an individual cavity of protein. The substate  $B$  answers to the residence of ligand inside the heme pocket (the cavity nearest to the iron on the distal side of heme). The rate constants  $k_{reb}$  and  $k_{esc}$  specify two competing processes: the irreversible heme-ligand rebinding for the ligand localized inside the heme pocket (that is, the transition from the substate  $B$  to the state  $A$ ) and the migration of unbound ligand between the heme pocket and other protein cavities (the transitions between  $B$  and the substates  $\{C_1, \dots, C_n\}$ ). Immediately after photodissociation the unbound ligand is in the substate  $B$ . Therefore the quantity  $k_{esc}$  can be associated with ligand escape from the pocket. In general, the GR is essentially determined by the specificities of heme-ligand interaction (including the spin restriction effect, the position and the orientation of ligand with respect to the heme plane) [5,11–13] and the effect of residues surrounding the heme [14–19]. Important factors for the heme-ligand rebinding are also the state of tertiary [2,20–22] and quaternary [2,23–25] structures of protein, the conformation transitions in protein [2,10,26–28] and the solvent impact [23,29–31]. As a consequence, the kinetic curve (that is, the probability  $P(t)$  to find the heme in unbound state) of GR is a non-exponentially decaying function of time [32–35]. After realization of the geminate stage a portion  $P_s$  of the hemes remains in unbound state:  $P_s \leq 0.01$  for  $NO$ ,  $P_s \sim 0.1 \div 0.2$  for  $O_2$  and  $P_s \sim 0.5 \div 1.0$  for  $CO$ . The quantity  $P_s$  characterizes the efficiency of ligand escape from the protein to the solvent.

Molecular dynamics simulations [11,36–40] show that the movement of unbound  $NO$ ,  $O_2$  or  $CO$  ligands in heme protein can be associated both with ligand trapping for a significant time in individual cavities and with rare jump-like transitions between adjacent cavities. It implies a fast establishment of equilibrium for the probability distribution of ligand within individual cavities. The establishment occurs on a time scale comparable to the mean time interval  $\tau_w$  between the collisions of ligand with cavity walls. At room temperatures the time  $\tau_w$  lies in the subpicosecond range ( $\tau_w \sim 0.1$  ps for  $NO$  in the heme pocket of  $Mb$  [41]). The ligand redistribution between protein cavities is observed on a longer time scale ranging from several tens of picoseconds ( $\sim 40$  ps for  $NO$  in  $Mb$  [41]) up to several tens of nanoseconds ( $\sim 50$  ns for

*CO* in *Hb* [42]). Unfortunately, in practice the detailed molecular dynamics simulation can not be implemented to the GR due to enormous computational efforts.

In the study we apply an alternative approach based on the diffusion approximation to ligand migration in protein. Such an approximation is valid for times  $t \gg \tau_w$  when the deterministic nature of ligand motion can be ignored. Here the interval  $\tau_w$  can be recognized as a correlation time. The diffusion-like character of ligand migration in the heme proteins can be a reason of the non-exponential temporal dependence for the probability  $P(t)$  [43–45]. For instance, a two-dimensional diffusion is demonstrated for *CO* in *Mb* [45] to explain the power-law kinetics to be observed in the experiment. Generally, reaction (1) can be represented in a three-dimensional diffusion approximation by equation

$$\frac{\partial n}{\partial t} = \nabla(D\nabla n) - R_{reb}n \quad (2)$$

with the diffusion coefficient  $D = D(x, y, z)$ . The quantity  $n = n(x, y, z, t)$  is the probability density of unbound ligand in the protein. The stepwise function  $R_{reb} = R_{reb}(x, y, z)$  specifies the heme-ligand rebinding and equals to  $k_{reb}$  inside the heme pocket or to zero otherwise.

In order to solve diffusion equation (2) and to follow the evolution of GR we use a simple model proposed recently in [46]. The model reproduces dynamics of random walk of particle in porous media (such, for instance, as glass-like matrices [47–49]) and takes into account an initial retention of ligand inside the heme pocket (that is, in the substate *B*). In the absence of heme-ligand rebinding the substate *B* is realized at times  $t < \tau_{esc}$  ( $\tau_{esc} = 1/k_{esc}$  is the time of ligand escape from the heme pocket to others cavities). Only on a longer time scale ( $t > \tau_{esc}$ ) the ligand succeeds to leave the pocket and to migrate over protein cavities. Due to the diffusion nature of the migration the time  $\tau_{esc}$  can be specified in terms of the diffusion coefficient  $D$ .

The approach is implemented with the help of a numerical simulation where the unbound ligand is represented by a structureless particle. For simplicity, in the simulation we make some assumptions. The ligand migration is assumed to be restricted to the distal side of heme. The ligand motion (realized on a short time scale  $t \leq \tau_w$ ) inside the heme pocket is represented by a unforced displacement of the particle within a restricted hemispheric region of space. At  $\tau_w \ll t \ll \tau_{esc}$  the ligand trajectories are effectively mixed in the configurational space, resulting in a homogeneous distribution for the ligand inside the cavities. Hence, the probability of irreversible heme-ligand rebinding is accepted to be uniform for the whole heme pocket. We take into account also that on the time scale  $t \gg \tau_w$  the fast intracavity displacements of ligand for the substates  $\{C_1, \dots, C_n\}$  do not influence essentially on the GR kinetics and can be ignored in the

simulation. Therefore the ligand displacement exterior to the heme pocket is simulated as a random walk (that is, as a Brownian-like motion) of the particle outside the hemispheric region. This walk is a spatially homogeneous diffusion with the diffusion coefficient  $D$ . We neglect also the structural transformations (such as a shift of the iron with respect to the porphyrin ring plane) at the conformational transition of protein between the unliganded and liganded states. According to the model, the temporal behavior for the probability  $P(t)$  can be specified in terms of two parameters: the time  $\tau_{esc}$  and the time  $\tau_{reb} = 1/k_{reb}$  of heme-ligand rebinding. The description of the model is represented in Section 2.

In order to demonstrate the usefulness of such an approach to the GR of heme proteins we apply the model to the analysis of available experimental data. We analyze the measured recombination kinetics and the efficiency for a postphotodissociative GR of human hemoglobin *HbA* [50,51]. These measurements were carried out at various *pH* values of the solution. Here we determine the times  $\tau_{reb}$  and  $\tau_{esc}$  as functions of *pH* and estimate the influence of solution properties on the heme-oxygen rebinding, the migration of oxygen molecule in hemoglobin and the efficiency of oxygen escape from the protein. The association of the times  $\tau_{reb}$  and  $\tau_{esc}$  with the time of a bimolecular recombination process for hemoglobin is analyzed. The results of simulation and their analysis are represented in Section 3.

## II. DIFFUSION-BASED MODEL OF GEMINATE RECOMBINATION

The movement of unbound ligand is considered in a Cartesian coordinate system  $xyz$  attached rigidly to the heme group of atoms. The system origin is superposed on an iron atom located in the middle of heme porphyrin ring. The  $x$  and  $y$  axes are aligned with the heme plane. The positive direction for the  $z$  axis corresponds to the distal side of heme. The ligand migration in protein is simulated as a probability redistribution for the ensemble of structureless particles over a three-dimensional hemispheric space with  $z > 0$ . As in [52], in our simulation the heme pocket is represented by a hemispheric region (designated here as a cage) of radius  $\rho$ . At an initial time instant the particle is uniformly distributed inside the cage.

The individual particle to be exposed to a sequence of  $\delta$ -shaped uncorrelated kicks executes a random walk in the space. As for the Brownian particle, each kick results in an abrupt change in the particle velocity. Between the kicks the particle is in unforced motion. On a time interval  $\Delta t_k = t_{k+1} - t_k$  ( $t_k$  is the time instant of action for  $k$ -th kick) between adjacent kicks the particle is specified by the velocity  $\mathbf{v}_k$  and the length  $L_k$  of free path (note that  $\Delta t_k = L_k/|\mathbf{v}_k|$ ). Then the radius vector  $\mathbf{r}(t_{k+1})$  of

particle for the time point of  $k+1$ -th kick can be obtained from iteration procedure

$$\mathbf{r}(t_{k+1}) = \mathbf{r}(t_k) + \frac{L_k \mathbf{v}_k}{|\mathbf{v}_k|} \quad (3)$$

where the radius vector  $\mathbf{r}(t_k)$  is given for the time instant of  $k$ -th kick. The projections  $v_{j,k}$  ( $j = x, y, z$ ) of the velocity  $\mathbf{v}_k$  onto the coordinate axes and the length  $L_k$  are accepted to be independent random quantities, new values of which are generated at each kick. The quantities  $v_{j,k}$  is obtained from the Maxwell distribution

$$P_M(v_{j,k}) = \sqrt{\frac{m}{2\pi kT}} \exp\left(-\frac{mv_{j,k}^2}{2kT}\right) \quad (4)$$

Here  $m$  is the particle mass and  $T$  is a protein temperature. At an attainment of the  $z = 0$  plane bounding the space, a new particle velocity with  $v_z > 0$  is regenerated in accordance with distribution (4).

The choice of free path length is dictated by the particle location in the space. Within the hemispheric cage the particle displacement is unforced and the particle undergoes no kicks. The length  $L_k$  is determined then from the ballistic trajectory of particle between the cage boundaries. In this case the length is comparable to the cage size  $\rho$ . We accept here that the mean time  $\tau_h = \langle \Delta t_{h,k} \rangle$ , during which the particle crosses the cage, can be associated with the time interval  $\tau_w$  between the collisions of ligand with heme pocket walls:  $\tau_h \sim \tau_w$ .

Exterior to the cage, the particle is exposed to uncorrelated kicks. The absence of correlation between the kicks implies that the quantity  $L_k$  is distributed according to the exponential law:

$$P(L_k) = \frac{1}{\lambda} \exp\left(-\frac{L_k}{\lambda}\right) \quad (5)$$

where  $\lambda = \langle L_k \rangle$  is the mean length of free path for the particle displacement outside of the cage. The mean time  $\tau_c$  between adjacent kicks and the length  $\lambda$  are related to the diffusion coefficient  $D = \langle L_k^2 \rangle / 6\tau_c$  by equations:

$$\tau_c = \frac{6mD}{\pi kT} \quad (6)$$

$$\lambda = 3D \sqrt{\frac{2m}{\pi kT}} \quad (7)$$

Thus, the spatial displacement of the particle is obtained from iterative equation of motion (3) and depends on the random sampling of variables  $v_{x,k}$ ,  $v_{y,k}$ ,  $v_{z,k}$  and  $L_k$ , the statistical distributions for which are specified by the parameters  $m/T$ ,  $D$  and  $\rho$ . As mentioned above, under the conditions typical for the heme proteins (that is, the temperature, the ligand mass and the distinctive sizes of heme pocket) the times  $\tau_c$  and  $\tau_h$  to be accepted here

as correlation times are negligibly short as compared to the characteristic times of GR. The length  $\lambda$  is essentially small as against the size  $\rho$  of hemispheric cage. Hence, the temporal behavior for the probability redistribution of ligand in heme protein can be described in terms of the diffusion-based approach.

Our model reproduces dynamics of ligand migration over protein cavities. Initially, the ligand is retained inside the heme pocket and the root-mean-square displacement  $S(t) = \sqrt{\langle |\mathbf{r}(t) - \mathbf{r}(0)|^2 \rangle}$  of ligand from the initial position does not exceed the characteristic size of the pocket. In a sense such a retention is analogous to the so called cage-effect to be observed for single atoms or small molecules in porous glass-like matrices [47–49]. The time scale, on which the retention is realized, is limited by a time point  $\tau_{esc}$ . This time is a lifetime for the ligand inside the heme pocket in the absence of rebinding and specifies thereby a ligand escape from the pocket. Only on a longer time scale (when the ligand succeeds to leave the pocket and to migrate over the protein) the ligand displacement  $S(t)$  starts to increase significantly. According to the model, we associate the time  $\tau_{esc}$  with the time of particle localization in the hemispheric cage. In the simulation the particle displacement  $S(t)$  does not exceed the cage radius  $\rho$  on the short time scale  $t < \tau_{esc}$ . At longer times the quantity  $S(t)$  increases with time. Due to the diffusion nature of the particle displacement the increase in  $S(t)^2$  is a linear function of time and  $S(t)^2 \approx 6Dt$  at  $t \gg \tau_{esc}$ . The relation between the time  $\tau_{esc}$  and the diffusion coefficient  $D$  can be then determined from the requirement  $\rho^2 \sim S(\tau_{esc})^2 = 6D\tau_{esc}$ :

$$\tau_{esc} = \frac{\rho^2}{6D} \quad (8)$$

Fig. 1 demonstrates a typical temporal dependence for the relative particle displacement  $S(t)^2/\rho^2$  simulated within the framework of our model. The displacement  $S(t)$  is shown in the figure to be constant ( $S(t) \sim \rho$ ) at  $\tau_h \ll t \ll \tau_{esc}$ . On a longer time scale ( $t \gg \tau_{esc}$ ) the quantity  $S(t)$  approaches asymptotically the diffusion law:  $S(t)^2 \approx 6Dt = t\rho^2/\tau_{esc}$ . Notice that for the time scale  $\tau_h \ll t \ll \tau_{esc}$  the temporal behavior of relative displacements  $S(t)/\rho$  is specified by the only parameter  $\tau_{esc}$ . In the following, we will adjust the parameter  $\tau_{esc}$  in the simulation. For definiteness, this adjustment will be carried out by means of variation in the diffusion coefficient  $D$ . The particle mass  $m$ , the temperature  $T$  and the cage radius  $\rho$  will take fixed values typical for the ligand and the protein.

The heme-ligand rebinding is accepted to be an irreversible process occurring when the ligand is localized inside the heme pocket. Therefore this process is simulated as a random 'death' for the particle within the hemispheric cage. The particle with  $|\mathbf{r}(t_k)| < \rho$  is 'obliterated' if  $\xi_k \leq \Delta t_{h,k}/\tau_{reb}$ . Here  $\xi_k$  is a random quantity

to be generated for each period  $\Delta t_{h,k}$  when the particle crosses the cage. The quantity  $\xi_k$  is distributed uniformly in the interval  $[0, 1]$ . The 'obliterated' particle is excluded from the following consideration.

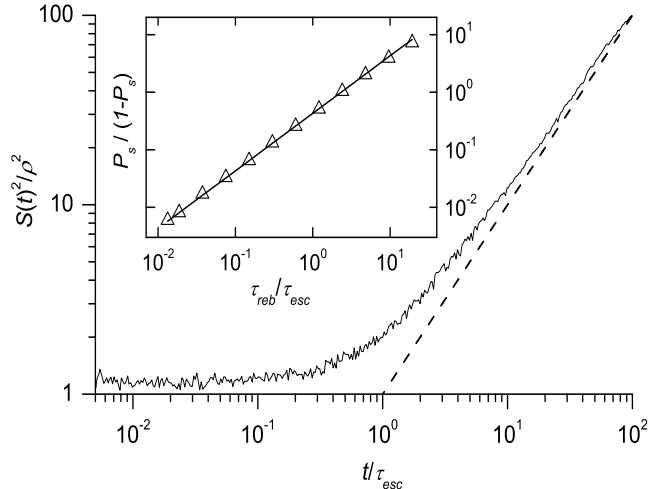


FIG. 1. A simulated temporal dependence for the mean-square relative displacement  $S(t)^2/\rho^2$  of particle from the initial position at  $m = 32$  amu,  $T = 300$  K,  $\rho = 4$  Å,  $D = 3.2 \cdot 10^{-11}$  m<sup>2</sup>/s (solid line). The dashed line shows dependence  $S(t)^2/\rho^2 = t/\tau_{esc}$  corresponding to the diffusion law. The inset shows the quantity  $P_s/(1 - P_s)$  as a function of the ratio  $\tau_{reb}/\tau_{esc}$ . ( $\Delta$  - our simulation at  $m = 32$  amu,  $T = 300$  K,  $\rho = 4$  Å). The solid line gives approximation (9) at  $C_s = 0.43$ .

The probability  $P(t)$  to find the heme in unbound state is found as the ensemble-averaged relative number of the 'non-obliterated' particles at a time instant  $t$ . In contrast to the relative displacement  $S(t)/\rho$ , the temporal behavior for the probability  $P(t)$  depends not only on the diffusion properties, but on the rate of heme-ligand re-binding as well. Hence, the behavior of  $P(t)$  can be specified in terms of the times  $\tau_{esc}$  and  $\tau_{reb}$ . In general, the probability  $P(t)$  is a monotonously decreasing function of time, which approaches asymptotically a steady value  $P_s$  at  $t \rightarrow \infty$ . This value gives a portion of the hemes remaining in unbound state after realization of GR. As in diffusion equation (2), in our model the quantity  $P_s$  is a function dependent merely on the ratio between  $\tau_{esc}$  and  $\tau_{reb}$ . The analysis of simulated data shows that for a wide range of values  $\tau_{esc}$  and  $\tau_{reb}$  satisfying the requirement  $\tau_{reb}/\tau_{esc} < 20$  (that is, under conditions typical for the GR) the best approximation of the dependence can be represented by relation

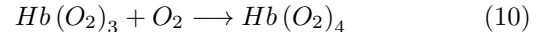
$$\frac{P_s}{1 - P_s} \approx C_s \frac{\tau_{reb}}{\tau_{esc}} \quad (9)$$

where the coefficient  $C_s$  is obtained from mean square fitting. At  $m = 32$  amu,  $T = 300$  K and  $\rho = 4$  Å the fitting gives a value  $C_s = 0.43$ . The inset of Fig. 1 demonstrates a good agreement between approximation

(9) and the simulated data.

### III. GEMINATE RECOMBINATION OF HUMAN HEMOGLOBIN WITH OXYGEN

We use the described model in order to analyze available experimental data for a postphotodissociative reoxygenation of human hemoglobin *HbA*. The data include the measured recombination kinetics and the efficiency of oxygen escape from the protein to the solvent for the monomolecular (geminate) and bimolecular stages of recombination reaction



going at room temperatures after fast laser-initiated breaking of a  $Fe - O_2$  bond [51,51]. The kinetic measurements are carried out with a time resolution of 10 ps for a time scale  $t < 1.5$  ns at different fixed  $pH$  values for the solution. The values of  $pH$  fall within an interval between 6.0 and 9.4:  $pH = \{6.0, 6.8, 7.0, 7.2, 7.7, 8.0, 8.5, 9.4\}$ .

According to the model, in the analysis of reoxygenation reaction (10) the temporal decay for the probability  $P(t)$  is interpreted as a result of two competing processes: the heme-oxygen re-binding for the oxygen molecule localized inside the heme pocket and the diffusion-like migration of the oxygen between hemoglobin cavities. Here we determine the times  $\tau_{reb}$  and  $\tau_{esc}$ , which specify the processes. We determine the times as functions of  $pH$  and analyze the effect of solution properties on the processes to be considered. Due to the tetramer arrangement of hemoglobin (the *Hb* molecule consists of heme containing  $\alpha$ - and  $\beta$ -chains) the observed kinetic curve represents a reoxygenation kinetics summarized over the chains. Here we make no distinction for reaction (10) between the  $\alpha$ - and  $\beta$ -chains and determine thereby chain-averaged times.

#### A. Reoxygenation kinetics for hemoglobin

The analysis of reoxygenation kinetics for the hemoglobin is based on the estimation of the times  $\tau_{reb}$  and  $\tau_{esc}$ . The times are found with the help of a numerical simulation, the iterative procedure for which is described above (see Section 2). In the simulation the masse of walking particle is accepted to equal the mass of oxygen molecule. The temperature  $T$  is 300K. The size  $\rho$  of hemispheric cage is 4 Å that corresponds to the time  $\tau_h < 1$  ps. The times  $\tau_{reb}$  and  $\tau_{esc}$  are chosen from an interval of values from 0.1 up to 5 ns. The correlation time  $\tau_c$  and the mean length  $\lambda$  of free path are determined by relations (6) and (7). They are negligibly small in comparison with  $\tau_{reb}$ ,  $\tau_{esc}$  or  $\rho$ . The simulated dependences for the probability  $P(t)$  are obtained from ensemble averaging for more than  $10^6$  particles.

In the simulation the parameters  $\tau_{reb}$  and  $\tau_{esc}$  are so adjusted that the ensemble-averaged temporal dependence of simulated probability  $P(t)$  is the best agreement with a measured kinetic curve. The agreement is specified by the relative root-mean-square deviation  $R$  between the simulated and experimental curves. The simulated dependence for  $P(t)$  is shown in Fig. 2 to reproduce well kinetic measurements on the considered time scale. The minimal deviation  $R$  achieved in our calculations for each of the fixed  $pH$  values does not exceed the measurement error ( $R \leq 0.01$ ). Such an agreement testifies that the non-exponential dependence for  $P(t)$  with time can be explained by a diffusion-like migration of ligand over protein matrix. Hence, the parameters  $\tau_{reb}$  and  $\tau_{esc}$  can be used for the analysis of the processes, which are responsible for the GR.

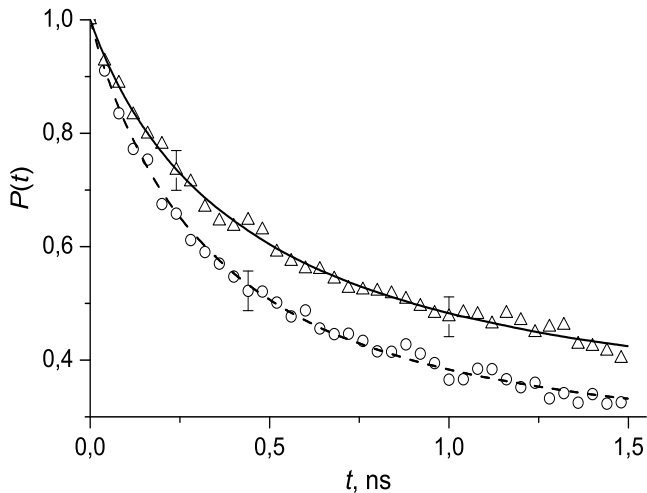


FIG. 2. A temporal dependence for the probability  $P(t)$  to find the heme in unbound state after fast breaking of a  $Fe - O_2$  bond in human hemoglobin  $HbA$  for the geminate stage of reaction (10) at  $pH = 6.0$  (solid line - our simulation with  $\tau_{reb} = 0.495$  ns and  $\tau_{esc} = 0.84$  ns,  $\Delta$  - experiment [50]) and 8.5 (dashed line - our simulation with  $\tau_{reb} = 0.366$  ns and  $\tau_{esc} = 0.92$  ns,  $\circ$  - experiment [50]).

The influence of solution properties on the migration and the rebinding of oxygen molecule in hemoglobin is assessed from a  $pH$  dependence for the obtained times  $\tau_{reb}$  and  $\tau_{esc}$ . Our simulation demonstrates a significant variation in the rate of heme-oxygen rebinding with  $pH$  (see Fig. 3). The increase of quantity  $pH$  from 6.0 to 8.5 results in a shortening for the time  $\tau_{reb}$  by a factor of 1.4 (from 0.5 down to 0.36 ns). With the following rise of  $pH$  to 9.4 the parameter  $\tau_{reb}$  appears to increase up to 0.4 ns. The minimum magnitude of  $\tau_{reb}$  is observed at  $pH = 8.5$ . Despite the considerable  $pH$  effect for the heme-oxygen rebinding, the variation in  $pH$  influences slightly on the oxygen escape from the heme pocket. The time  $\tau_{esc}$  is shown in Fig. 3 to be within a range of values from 0.82 to 0.92 ns and to be weakly dependent on  $pH$ . The

$pH$ -averaged magnitude of  $\tau_{esc}$  is approximately 0.88 ns. Notice that this magnitude is larger than  $\tau_{reb}$  by a factor of 2 ÷ 3.

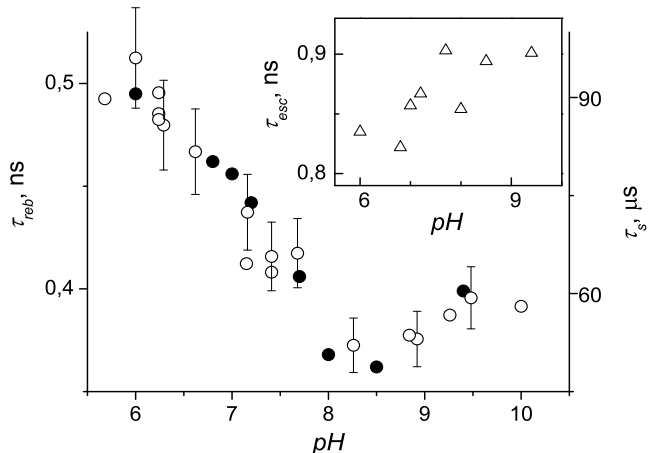


FIG. 3. The times of heme-oxygen rebinding as functions of  $pH$  for the geminate ( $\tau_{reb}$ , full circles - our simulation) and bimolecular ( $\tau_s$ ,  $\circ$  - experiment [50,51]) stages of recombination reaction (10). The inset shows the  $pH$ -dependence ( $\Delta$ ) obtained in our simulation for the time  $\tau_{esc}$  of oxygen escape from the heme pocket of  $HbA$ .

The obtained values for the times  $\tau_{reb}$  and  $\tau_{esc}$  are in good agreement with the experimental study of the alkaline Bohr effect (the variation of the recombination rate  $1/\tau_s$  with  $pH$  for the bimolecular stage of GR) [50,51]. The behavior of  $pH$ -dependence for the time  $\tau_{reb}$  is demonstrated in Fig. 3 to be similar to one for the time  $\tau_s$  of bimolecular rebinding. Such an agreement testifies that for the monomolecular GR the variation of the rebinding rate with  $pH$  can be associated with the same structural transformation as for the bimolecular stage of reaction (10). Histidine imidazoles of  $C$ -terminal sites and  $\alpha$ -amides of  $N$ -terminal sites seem to be the aminoacid residues, which are responsible for this transformation [2,8,53]. Specifically, in the alkaline Bohr effect the interaction between the solvent and the  $\beta 146His$  residue (a  $C$ -terminal histidine of  $\beta$ -chain) is one of the most probable reasons for the heme structure modification and the rearrangement of neighboring aminoacid residues [2]. Our simulation confirms that the variation in  $pH$  can result in essential structural transformations in immediate proximity from the iron atom. The strong  $pH$ -dependence for the times  $\tau_{reb}$  and  $\tau_s$  is a consequence of the transformations.

The ligand penetration from the solvent into the heme pocket is shown for  $O_2$  or  $NO$  in  $Hb$  [5] to be a process restraining the rate of bimolecular recombination (10). Therefore, the similarity between the  $pH$ -dependences for  $\tau_{reb}$  and  $\tau_s$  testifies that the change in  $pH$  has a slight effect on the oxygen migration in hemoglobin at the mono- and bimolecular stages of recombination (10). The weak  $pH$ -dependence for the obtained times of oxy-

gen escape from the pocket confirms this assumption. Such a  $pH$ -invariant behavior for the oxygen migration can be interpreted by the independence of mobility for the hemoglobin side chains (which seem to be responsible for the ligand transitions between cavities of heme protein [38]) on  $pH$  of the solution.

### B. Efficiency of oxygen escaping from hemoglobin

The obtained times  $\tau_{reb}$  and  $\tau_{esc}$  are used then in order to estimate the efficiency of oxygen escape from hemoglobin as a function of  $pH$ . The efficiency is proportional to the quantum yield of photodissociation and can be associated with the portion  $P_s$  of the hemes remaining in unbound state after realization of the geminate reoxygenation stage [54]. In our simulation the ratio  $\tau_{reb}/\tau_{esc}$  falls within a range of values from 0.4 up to 0.6. It implies that the portion  $P_s$  can be determined from approximation(9). The behavior of  $pH$ -dependence for the obtained quantity  $P_s$  agrees well with one for the measured quantum yield of photodissociation [51,51]. The quantity  $P_s$  is shown in Fig. 4 to be proportional to the apparent quantum yield  $\gamma$  for the whole investigated scale of  $pH$ .

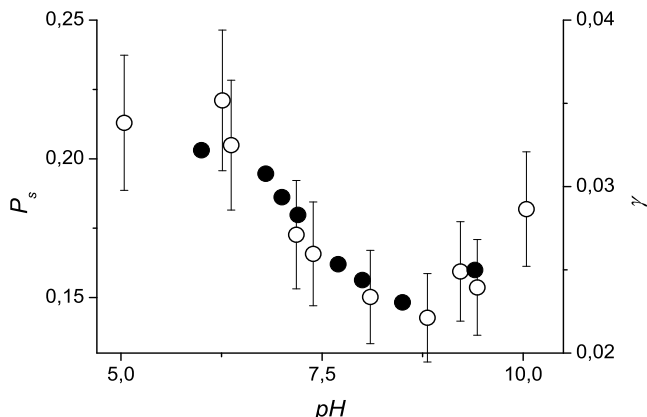


FIG. 4. The portion  $P_s$  of the hemes remaining in unbound state after realization of the geminate stage of *HbA* reoxygenation (10) (full circles - our simulation) and the apparent quantum yield  $\gamma$  of *HbA* photodissociation ( $\circ$  - experiment [50,51]) depending on  $pH$  values of the solution.

Notice that for the studied range of  $pH$  values the quantity  $C_s\tau_{reb}/\tau_{esc}$  is considerably low in comparison with 1 ( $C_s\tau_{reb}/\tau_{esc} \sim 0.15 \div 0.25$ ) and the time  $\tau_{esc}$  is practically constant. Therefore the relation of the portion  $P_s$  with the time  $\tau_{reb}$  is close to the linear law:

$$P_s = \frac{C_s\tau_{reb}}{(\tau_{esc} + C_s\tau_{reb})} \approx C_s \frac{\tau_{reb}}{\tau_{esc}} \propto \tau_{reb}. \quad (11)$$

In our study (see Fig. 3 and Fig. 4) the  $pH$ -dependences obtained for  $P_s$  and  $\tau_{reb}$  are similar that testifies again

that the transport properties for the oxygen molecule in hemoglobin do not depend on  $pH$ .

### C. Diffusion properties of oxygen migration in hemoglobin

The analysis of X-ray diffraction data [55,56] for oxygenated and deoxygenated species of human hemoglobin (PDB ID *1HHO* and *2HHB*, correspondingly) shows that the cage radius  $\rho$  to be associated with the heme pocket size is a quantity ranging from 1 up to 5 Å (taking into account the Van der Waals radiuses). Hence, the diffusion coefficient  $D$  for the oxygen migration in hemoglobin can be estimated from relation (8):  $D = \rho^2/6\tau_{esc} \sim 0.2 \div 5 \cdot 10^{11}$  m<sup>2</sup>/s. This coefficient is intermediate to diffusion coefficients for small molecules in water ( $10^{-9}$  m<sup>2</sup>/s) and solids ( $10^{-18}$  m<sup>2</sup>/s at  $T < 400K$ ) [57]

According to the diffusion law, at a time instant  $t_m$  the root-mean-square displacement  $\sqrt{\langle |\mathbf{r}(t)|^2 \rangle}$  of the ligand from the iron is approximately equal to  $\rho\sqrt{t_m/\tau_{esc}}$ . It implies that on the completion of kinetic measurements ( $t_m = 1.5$  ns [50]) the oxygen remains inside the protein and is localized in immediate proximity from the heme pocket:  $\sqrt{\langle |\mathbf{r}(t)|^2 \rangle} \approx 1.3\rho < 7$  Å. This conclusion is consistent with results of spectroscopy investigation of motional dynamics for *CO* in *Hb* [42].

## IV. CONCLUSION

We have represented a simple model of the geminate recombination of heme proteins with small ligands. The model takes into account dynamic properties of ligand displacement in protein matrix. In the model the recombination is due both to the heme-ligand rebinding and to the diffusion-like migration of ligand between protein cavities. The temporal behavior for the probability  $P(t)$  to find the heme in unbound state is specified in terms of two parameters. They are the time  $\tau_{reb}$  of heme-ligand rebinding for the ligand inside the heme pocket and the time  $\tau_{esc}$  of ligand escape from the pocket.

We have applied our model in order to analyze a postphotodissociative geminate reoxygenation of human hemoglobin at various  $pH$  values of the solution. The measured kinetic curves and the efficiency of oxygen escape from the hemoglobin are well reproduced in our simulation. It testifies that the non-exponential behavior for the probability  $P(t)$  can be explained by a diffusion-like migration of ligand over protein cavities. This conclusion is consistent with recent kinetic measurements [58]. We believe that the theory-experiment agreement may be considered as an additional validation for the glass-like model of proteins.

Our study demonstrates also that the variation in  $pH$  can result in considerable changes for the rate of heme-ligand rebinding. At the time, the oxygen migration in hemoglobin depends slightly on  $pH$ . We have interpreted this effect as a result of essential structural transformations in immediate proximity from the iron atom. Certainly, this conclusion demands a more detailed and thorough examination. In any case we suppose that the  $pH$ -induced modification of the initial stage of GR (if the modifications are observed) can be explained by a change in the rate of heme-ligand rebinding.

- 
- [1] E. Antonioni and M. Brunori, Hemoglobin and myoglobin in their reactions with ligands, (North-Holland, Amsterdam, 1971).
- [2] M.F. Perutz, A.J. Wilkinson, M. Paoli and G.G. Dodson, Annu. Rev. Biophys. Biomol. Struct. 27 (1998) 1.
- [3] W.A. Eaton, E.R. Henry, J. Hoffrichter and A. Mozarelli, Nat. Struct. Biol. 6 (1999) 351.
- [4] D.A. Chernoff, R.M. Hochstrasser and A.W. Steel, Proc. Natl. Acad. Sci. USA. 77 (1980) 5606.
- [5] J.S. Olson, R.J. Rohlfs and Q.H. Gibson, J. Biol. Chem. 262 (1987) 12930.
- [6] X. Ye, A. Demidov and P.M. Champion, J. Am. Chem. Soc. 124 (2002) 5914.
- [7] G. Dadusc, J.P. Ogilvie, P. Shulenberg, U. Marvet and R.J.D. Miller, Proc. Natl. Acad. Sci. USA 98 (2001) 6110.
- [8] N.N. Kruk, Ph.D. Thesis, Institute of Molecular and Atomic Physics, NASB, Belarus (1996).
- [9] B.M. Dzhagarov, J. Appl. Spectr. 66 (1999) 516.
- [10] H. Frauenfelder, F. Parak and R.D. Young, Ann. Rev. Biophys. Chem. 17 (1988) 451.
- [11] D.A. Case and M. Karplus, J. Mol. Biol. 132 (1979) 343.
- [12] Q.H. Gibson, J.S. Olson, R.E. McKinnie and R.J. Rohlfs, J. Biol. Chem. 261 (1986) 10228.
- [13] Yu.A. Berlin, N.I. Chekunaev and V.I. Goldanskii, Chem. Phys. Letters 197 (1992) 81.
- [14] W.T. Potter, M.P. Tucker, R.A. Houtchens and W.S. Caughey, Biochemistry 26 (1987) 4699.
- [15] J.M. Rifkind, Hemoglobin (Elsevier, New-York, 1988).
- [16] A. Bruha and J.R. Kincaid, J. Am. Chem. Soc. 110 (1989) 6006.
- [17] B.A. Springer, S.G. Sligar, J.S. Olson and G.N.Jr. Phillips, Chem. Rev. 94 (1994) 699.
- [18] J.A. Lukin, V. Simplaceanu, M. Zou, N.T. Ho and C. Ho, Proc. Natl. Acad. Sci. USA 97 (2000) 10354.
- [19] T.K. Das, M. Couture, Y. Quellet, M. Guertin and D.L. Rousseau, Proc. Natl. Acad. Sci. USA 98 (2000) 479.
- [20] S. Dasgupta and T.G. Spiro, Biochemistry 20 (1986) 5941.
- [21] K.R. Rodgers, C. Su, S. Subramaniam and T.G. Spiro, J. Am. Chem. Soc. 114 (1992) 3697.
- [22] S. Kimanaka and T. Kitagawa, J. Am. Chem. Soc. 114 (1992) 3256.
- [23] J. Baldwin and C. Chothia, J. Mol. Biol. 129 (1979) 175.
- [24] R.J. Morris and Q.H. Gibson, J. Biol. Chem. 259 (1984) 365.
- [25] L.P. Murray, J. Hoffrichter, E.R. Henry and W.A. Eaton, Proc. Natl. Acad. Sci. USA 85 (1988) 2151.
- [26] M. Lim, T.A. Jackson and P.A. Anfinrud, Proc. Natl. Acad. Sci. USA 90 (1993) 5801.
- [27] J.B. Johnson, D.C. Lamb, H. Frauenfelder, J.D. Muller, B.H. McMahon, G.U. Nienhaus and R.D. Young, Biophys. J. 71 (1996) 1563.
- [28] H. Frauenfelder, B.H. McMahon, R.H. Austin, K. Chu and J.T. Groves, Proc. Natl. Acad. Sci. USA 98 92001) 2370.
- [29] C. Ho and I.M. Russi, Biochemistry 26 (1987) 6299.
- [30] P.J. Steinbach, R.J. Loncharich and B.R. Brooks, Chem. Phys. 158 (1991) 383.
- [31] J.D. Muller, B.H. McMahon, E.Y.T. Chien, S.G. Sligar and G.U. Nienhaus, Biophys. J. 77 (1999) 1036.
- [32] A. Ansari, J. Berendzen, D. Braunstein, B.R. Cowen, H. Frauenfelder, M.K. Hong, I.E.T. Iben, T.B. Johnson, P. Ormos, T.B. Sauke, R.Scholl, A. Schulte, P.J. Steinbach, J. Vittitow and R.D. Young, Biophys. Chem. 26 (1987) 337.
- [33] J.W. Petrich, J.C. Lambry, K. Kuczera, M. Karplus, C. Poyart and J.L. Martin, Biochemistry 30 (1991) 3975.
- [34] P.J. Steinbach, A. Ansari, J. Berendzen, D. Braunstein, D. Chu, B.R. Cowen, D. Ehrenstein, H. Frauenfelder, T.B. Johnson, D.C. Lamb, S. Luck, J.R. Mourant, G.U. Nienhaus, P. Ormos, R. Philipp, A. Xie and R.D. Young, Biochemistry 30 (1991) 3988.
- [35] K. Kuczera, J.-C. Lambry, J.-L. Martin and M. Karplus, Proc. Natl. Acad. Sci. USA 90 (1993) 5805.
- [36] E.R. Henry, M. Levitt and W.A. Eaton, Proc. Natl. Acad. Sci. USA 82 (1985) 2034.
- [37] J. Kottalam and D.A. Case, J. Am. Chem. Soc. 110 (1988) 7690.
- [38] R. Elber and M. Karplus, J. Am. Chem. Soc. 112 (1990) 9161.
- [39] J.E. Straub and M. Karplus, Chem. Phys. 158 (1991) 221.
- [40] Q.H. Gibson, R.Regan, R.Elber, J.S.Olson and T.E. Carver, J. Biol. Chem. 267 (1992) 22022.
- [41] O. Schaad, H.-X. Zhou, A. Szabo, W.A. Eaton and E.R. Henry, Proc. Natl. Acad. Sci. USA 90 (1993) 9547.
- [42] P.A. Anfinrud, C. Han and R.M. Hochstrasser, Proc. Natl. Acad. Sci. USA 86 (1989) 8387.
- [43] B.B. Hasinoff, J. Phys. Chem. 85 (1981) 526.
- [44] L. Lindqvist, S. El Moshni, F. Tfibel, B. Alpert and J.C. Andre, Chem. Phys. Letters 79 (1981) 525.
- [45] M.C. Marden, Eur. J. Biochem. 128 (1982) 399.
- [46] V.S. Starovoitov, B.M. Dzhagarov, Chemical Physics (Moscow) 22 (2003) in press.
- [47] R. Yamamoto and A. Onuki, Phys. Rev. E. 58 (1998) 3515.
- [48] P. Gallo, M. Rovere, M.A. Ricci, C. Hartnig and E. Spohr, Europhys. Letters 49 (2000) 183.
- [49] J. Horbach and W. Kob, Phys. Rev. B. 60 (1999) 3169.
- [50] B. M. Dzhagarov, N.N. Kruk, S.A. Tikhomirov and V.A. Galievsky, in: Ultrafast processes in spectroscopy, eds. O. Svelto, S. de Silvestri and G. Denardo (New-York, Plenum Press, 1996).

- [51] B. M. Dzhagarov and N.N. Kruk, *Biofizika* 41 (1996) 606.
- [52] N.J. Cotes and M.G. Sceats, *Chem. Phys. Letters* 141 (1987) 405.
- [53] M.F. Perutz, J.V. Kilmartin, K. Nishikura, J.H. Fogg, P.J. Butler and H.S. Rollema, *J. Mol. Biol.* 138 (1980) 649.
- [54] B.M. Dzhagarov, V.S. Chirvonyi and G.P. Gurinovich, in: *Laser Picosecond Spectroscopy and Photochemistry of Biomolecules*, ed. V.S. Letokhov, (Bristol, IOP Publishing Ltd., 1987).
- [55] B. Shaanan, *J. Mol. Biol.* 171 (1983) 31.
- [56] G. Fermi, M.F. Perutz, B. Shaanan and R. Fourme, *J. Mol. Biol.* 175 (1984) 159.
- [57] G. Jost, *Diffusion in Solids, Liquids, Gases*, (New-York, Academic Press, 1952).
- [58] S.V. Lepeshkevich, N.V. Konovalova and B.M. Dzhagarov, *Biochemistry (Moscow)*, 68 (2003) in press